

Investigating the Hubble Constant Tension - Two Numbers in the Standard Cosmological Model

WEIKANG LIN ¹, KATHERINE J. MACK ¹, AND LIQIANG HOU¹¹Physics Department, North Carolina State University, Raleigh, NC 27695, USA

ABSTRACT

The current Hubble constant tension is usually presented by comparing constraints on H_0 only. However, the post-recombination background cosmic evolution is determined by two parameters in the standard Λ CDM model, the Hubble constant (H_0) and today's matter energy fraction (Ω_m). If we therefore compare all constraints individually in the H_0 - Ω_m plane, (1) various constraints can be treated as independently as possible, (2) single-sided constraints are easier to consider, (3) compatibility among different constraints can be viewed in a more robust way, and (4) whether or not a nonstandard model is able to reconcile all constraints in tension can be seen more effectively. We perform a systematic comparison of independent constraints in the H_0 - Ω_m space based on a flat Λ CDM model. Constraints along different degeneracy directions consistently overlap in one region of the space, with the exception of the local measurement from Cepheid variable-calibrated supernovae. Due to the different responses of individual constraints to a modified model, it is difficult for nonstandard models with modifications at high-, mid- or low-redshifts to reconcile all constraints if none of them have unaccounted-for systematic effects. Based on our analysis, the local measurement is the most outlying and therefore drives the bulk of the tension. This may suggest that the most likely solution to the tension is an alteration to the local result, either due to some previously unseen feature in our local cosmic environment, or some other unknown systematic effect.

Keywords: Cosmology, the Hubble constant tension, nonstandard cosmological models

1. INTRODUCTION

Cosmology used to be called “a search for two numbers,” referring to the Hubble constant and the deceleration parameter (Sandage 1970). While the former describes today's cosmic expansion rate and, when first discovered, caused Einstein to abandon his idea of the cosmological constant Λ , the latter turned out to be negative and prompted physicists to bring Λ back. Dubbed (flat) “ Λ CDM,” the simplest cosmological model fully determines the dynamics of the homogeneous universe with another combination of two numbers, this time pairing the Hubble constant H_0 with today's matter energy fraction Ω_m . Together with its description of large-scale inhomogeneities, this model has successfully explained various cosmological and astronomical observations. Its simplicity and (at least overall) concordance has made it the standard cosmological model, even while named after its two most mysterious aspects. The two numbers, H_0 and Ω_m , are the focus of this work.

Despite its successes, some tensions have recently been reported between observations based on the standard cosmological model. Among them, the Hubble constant tension is one of the most hotly debated: the local determination of H_0 based on Cepheid variable-calibrated Type Ia super-

novae (SNe) (Riess et al. 2019) is higher than the one inferred from cosmic-microwave-background (CMB) observations (Planck Collaboration et al. 2018) at a $4.4\text{-}\sigma$ confidence level, a discrepancy that has kept increasing with more precise data from both sides in the past decade. For the time being, it is unclear whether this tension is caused by some new physics beyond the standard cosmological model, or some systematic effects in either or both of the measurements.

Looking for other independent observations is important and pressing, as this can help us to draw a more robust conclusion on the cause of the H_0 tension. Unfortunately, most other constraints on H_0 are not currently precise enough to settle the question, and their model dependences make the comparison more difficult to interpret. Nonetheless, Λ CDM can be taken as the default model to which all others can be compared. And because there are two parameters (H_0 and Ω_m) that specify the background evolution in Λ CDM, we should not compare constraints only on H_0 . It is more instructive to perform a comparison in the H_0 - Ω_m space. The benefits of this have frequently been overlooked in the literature. Usually, in order to obtain stronger constraints on H_0 , different observations are combined to break degeneracies. Doing this not only reduces the number of constraints to compare, but also causes the joint results to correlate with each other as certain constraints are frequently used to break degeneracies (e.g., SNe). The model dependence of a joint result gets more complicated as well, because a new model

may change only some constraints in a joint study but not the others. We will take a different approach and treat constraints separately. In the H_0 - Ω_m space, several constraints are actually not weak compared to the local determination, because their favored parameter spaces are relatively small. Considering observations individually can allow us to treat constraints as independently as possible and to more clearly see which constraint in the H_0 - Ω_m plane would be altered in a nonstandard model, providing information on whether a proposed model can reconcile all constraints. Instead of just one parameter, a two-parameter comparison provides a fresh look at the H_0 tension and allow us to draw a more robust conclusion. In addition, general single-sided constraints are easier to include in the H_0 - Ω_m plane. We will show those advantages here and investigate the current H_0 tension with a systematic comparison of different constraints. We then discuss whether any nonstandard models are capable of reconciling all constraints, assuming systematic effects are not biasing any results.

2. METHODS AND RESULTS

In order to perform a systematic multi-constraint comparison, we have collected a number of independent constraints in the H_0 - Ω_m space obtained from different observations, assuming the standard flat Λ CDM model. We list them below.

- **Time-delay strong lensing (TDSL)** - the time-delay distance for strong lensing systems. This is insensitive to the underlying model. The TDSL constraint here is obtained by running the jupyter notebook provided in <https://shsuyu.github.io/H0LiCOW/site/>;
- **Type-Ia supernovae Pantheon (SN P)** - the relative change of the apparent magnitude of these standard candles as a function of redshift to constrain, e.g., Ω_m (Scolnic et al. 2018);
- **γ -ray attenuation (γ -ray)** - the optical depth along the light of sight depends on the cosmic evolution (Domínguez et al. 2019, chains obtained from private conversation);
- **Dark Energy Survey Year 1 (DES)** - correlations among galaxies and cosmic shear (3×2 correlation functions) (Abbott et al. 2018, chains obtained from <https://des.ncsa.illinois.edu/>);
- **Cosmic chronometers (CC)** - The differential ages of passively evolving galaxies at two nearby redshifts directly measure the cosmic expansion rate at that redshift. The constraint here is obtained by performing a likelihood analysis of the data compilation provided in Yu et al. (2018);
- **BAO at low redshift + BBN (BAO Low)** - baryon acoustic oscillations at $z_{\text{eff}} = 0.106$ (Beutler et al. 2011), 0.15 (Ross et al. 2015), 0.38, 0.51 and 0.61 (Alam et al. 2017);
- **BAO at high redshift + BBN (BAO High)** - baryon acoustic oscillations at $z_{\text{eff}} = 1.52$ (Ata et al. 2018) and 2.35 (Blomqvist et al. 2019, $\text{Ly}\alpha$ auto and $\text{Ly}\alpha \times \text{QSO}$). The two BAO constraints are obtained by running the corresponding modules in COSMOMC (Lewis & Bridle 2002) with BBN data (Cooke et al. 2018) constraining $\Omega_b h^2$;
- **WMAP 2013 (WMAP)** - 9-year Wilkinson Microwave Anisotropy Probe CMB data (Hinshaw et al. 2013);

- **Planck 2018 (Planck)** - full-mission Planck CMB temperature and polarization data (Planck Collaboration et al. 2018). Chains of both WMAP and Planck are obtained from <http://pla.esac.esa.int/pla/#home>;
- **Cepheid-calibrated SNIa (CV SN)** - local determination of H_0 using Type Ia SNe calibrated by Cepheid variables (Riess et al. 2019);
- **Cosmic age** - The cosmic time since $z = 100$ (t_{age}^{100}) should be larger than some estimated stellar ages (t_*)¹. For the orange bound in Figure 1, we use $t_* = 13.535 \pm 0.002$ Gyr for J18082002-5104378 (Schlaufman et al. 2018). Besides that, HD 140283 has an estimated age of 14.46 ± 0.8 Gyr (Bond et al. 2013). Some Galactic globular clusters also have high estimated ages, e.g., 13.4 ± 1.3 Gyr for NGC 5466 and 13.4 ± 1.5 Gyr for NGC 2298, NGC 6101 and NGC 6341 (O'Malley et al. 2017, Table 6). Although the uncertainties on other globular cluster ages are large, the mean values are consistently higher than $t_{\text{age}}^{100} \simeq 12.7$ Gyr as suggested by a Λ CDM universe with $H_0 \simeq 74$ km/s/Mpc and $\Omega_m \simeq 0.3$.

We present all the above constraints in Figure 1. To check the consistency of a number of constraints, it is instructive to consider whether there is some common parameter region simultaneously overlapped by them. Note that, when compared in the H_0 - Ω_m space, it is not necessary for the observations to give strong constraints on H_0 . For example, SN P is uninformative on H_0 , and the stellar age constraint is only single-sided. Observations only have to give some favored parameter space. Among those constraints, while the local determination is model independent and the TDSL technique is insensitive to a cosmological model, other constraints are model dependent. However, being model independent does not mean being free from systematic effects, which may affect any result. A multi-constraint comparison puts all constraints on similar footing.

We can see in Figure 1 that most constraints overlap at a common parameter space indicated by the guiding white and dashed circle. We stress that this circle is a guide, *not* a joint constraint. Importantly, the overlapping constraints are along different degeneracy directions, which more robustly shows that those constraints are consistent with each other. This point cannot be seen from a comparison of constraints on H_0 alone. The only constraint that lies outside the white dotted circle is CV SN, which overlaps with a subset of the constraints at different parameter regions. Roughly speaking, it overlaps with BAO Low at $\Omega_m \sim 0.4$; with SN P and DES at $\Omega_m \sim 0.3$; with BAO High, CC, γ -ray attenuation and WMAP at $\Omega_m \sim 0.23$; and with the cosmic-age bound below $\Omega_m \lesssim 0.25$.

It is useful to find a numerical way to quantify and generalize the above multi-constraint comparison. To do that

¹ We assume no stars could have formed before $z = 100$. A larger limiting redshift does not change the bound significantly. But a larger confirmed stellar age or a later stellar formation time will tighten the bound towards a smaller- H_0 or smaller- Ω_m direction.

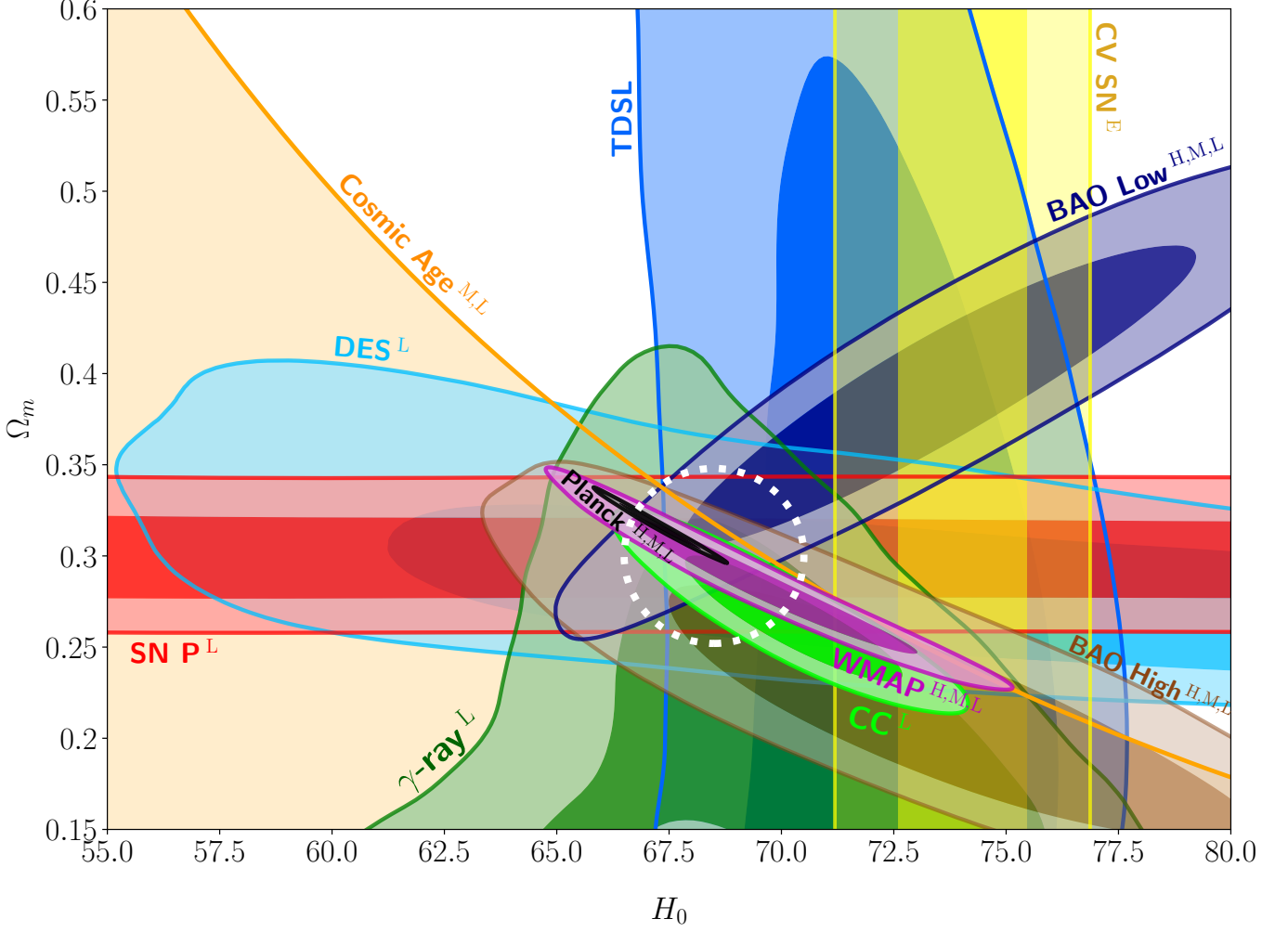


Figure 1. Different constraints in the H_0 and Ω_m space based on a flat Λ CDM model. Dark and light contours show the 68% and 95% confidence regions of each posterior. Parameter space outside the orange region is excluded by the cosmic-age bound. Most constraints with different degeneracy directions consistently overlap on the region indicated by the guiding white dashed circle. Note that the circle *does not* represent a joint constraint. Such a common region is however not overlapped by the Cepheid-based local determination of H_0 (CV SN). Contours correspond to SN P (red), BAO Low (brown), BAO High (navy), γ -ray (dark green), CC (light green), TDSL (blue), DES (light blue), WMAP (magenta), Planck (black), CV SN (yellow) and cosmic age ($t_{\text{age}}^{100} > 13.535$ Gyr; orange). See the text for descriptions and sources of those constraints. Each constraint in the figure is labeled according to whether they can be changed by nonstandard high- z models (H), mid- z models (M), low- z models (L), or local environmental factors (E). See the text for the definition of those model categories. We leave the TDSL technique without a label because it is relatively insensitive to the underlying cosmological model.

we use the momentum-based multi-dataset Index of Inconsistency (IOI) (Lin & Ishak 2017) and the associated “outlier index” (\mathcal{O}_j) (Lin & Ishak 2019),

$$\mathcal{O}_j \equiv \frac{1}{2} [N_d \text{IOI} - (N_d - 1) \text{IOI}^{(j)}], \quad (1)$$

where N_d is the number of constraints and $\text{IOI}^{(j)}$ is the multi-dataset IOI for the $(N_d - 1)$ constraints excluding the j th one. Given a set of constraints, IOI quantifies their overall inconsistency and \mathcal{O}_j tells us how incompatible each constraint is with the others. We show the results in Table 1. If one constraint has an \mathcal{O}_j that is significantly high compared to the others’, that constraint is outlying. This is the case for CV

SN, as shown in first row of Table 1. The second row shows that removing CV SN from the constraint set reduces the IOI and all \mathcal{O}_j ’s, indicating that the other constraints are, overall, consistent with each other. Note that it is important for the constraints to be obtained from different types of observations, to avoid the possibility that some or most of them suffer from the same type of systematic effects. Planck and WMAP are both CMB observations, and may have similar systematic effects. But removing WMAP from the constraint set and redoing the analysis gives similar results, as shown in the third row compared to the first. Both the constraint comparison shown in Figure 1 and this numerical analysis point

Table 1. Multi-dataset IOIs and \mathcal{O}_j ’s for our considered constraints (not including the cosmic-age bound). If one constraint has a significantly higher \mathcal{O}_j than the others, it is considered outlying. The first row is the analysis of all constraints, while the second and third are those after removing CV SN and WMAP, respectively. The last row is the results after replacing CV SN with the TRGB result (Freedman et al. 2019).

(IOI) & \mathcal{O}_j	CV SN	Planck	BAO (L)	BAO (H)	others
All (3.21)	7.63	3.91	2.16	1.41	<1.1
CV-SN (1.87)	N/A	1.97	1.46	1.63	<1.5
WMAP (3.54)	7.80	3.80	2.09	1.43	<1.1
TRGB CV-SN (1.75)	N/A	2.17	1.54	1.59	<1.4

to our conclusion that the local measurement is the strongest driver of the Hubble tension.

It is worth pointing out that the second most incompatible constraint is Planck, although with a much lower level of inconsistency than that of CV SN. This can be seen from the second row in Table 1, which shows that Planck has the highest \mathcal{O}_j after removing CV SN. We note that aside from the current H_0 tension, the inferred σ_8 from Planck is also higher than most large-scale-structure (LSS) results (Wibking et al. 2019; Joudaki et al. 2019), although it is not always the case (Hamana et al. 2019). Investigating the σ_8 tension is beyond the scope of this work, but it is possible that the two tensions are somehow related. Addison et al. (2016) has pointed out that the Planck small-scale CMB spectrum drives the parameter constraint toward a lower H_0 (below 70 km/s/Mpc), a higher σ_8 (above that of most LSS results), and a higher Ω_m than that of the SN P result, but see (Planck Collaboration et al. 2016) for a discussion arguing that these issues have been addressed. Nonetheless, we find that the Planck constraint does not on its own drive the current H_0 tension.

3. NONSTANDARD COSMOLOGY

Our analysis, above, examines the consistency of current constraints assuming a flat, Λ CDM model with no new physics. It is frequently suggested that an alternative cosmological model may be found that could reconcile all of the above constraints. A plethora of models have been proposed in the literature. While a detailed discussion of each model is beyond our scope here, we provide a general discussion of how high- z , mid- z , and low- z nonstandard models as well as local environmental factors can alter constraints. It is important to note that any proposed model can usually change only a subset of constraints. This is another advantage of comparing constraints individually instead of comparing combinations of subsets of them: it is easier to see which constraints can be changed in a proposed model. In Figure 1, we label each constraint by “H” (high- z), “M” (mid- z), “L” (low- z) or “E” (local/ environmental) according to whether it can be changed by the corresponding models/proposals. (The TDSL technique is relatively insensitive to the underlying cosmological model if the redshifts of the systems are not too high,

so we leave it without a label.) We will discuss whether those models/proposals can reconcile all the constraints in tension.

High- z models (H) here refer to those have some non-standard physics before or around recombination, but reduce to a Λ CDM universe thereafter (e.g., by $z \sim 100$). Examples are early-time dark energy (Poulin et al. 2019) and self-interacting neutrinos (Kreisch et al. 2019). Models of this category usually inject some extra energy before recombination, making the baryon-photon plasma sound horizon smaller. To compensate for this change and to match the observed angular size of the sound horizon, the Hubble constant needs to be higher than the CMB-inferred value in the Λ CDM model. Also, there is a “theoretical correlation” between the late-time BAO and the CMB observations in the sense that they both involve the calculation of the baryon-acoustic-oscillation sound horizon (although at two different epochs)². It is therefore also possible for high- z models to reconcile the late-time BAO constraints with CV SN. However, since these models reduce to a Λ CDM universe after recombination, they cannot change the constraints from late-time observations, especially those from γ -ray attenuation, cosmic chronometers, cosmic age, and the Pantheon supernovae. There would still be no commonly overlapping region in the H_0 - Ω_m space for CV SN and those late-time constraints. In particular, the stronger the cosmic-age bound, the higher the pressure would be upon models of this category.

Mid- z models (M) refer to those have some non-standard physics after recombination but before $z \sim 6$. An example is fractional decaying dark matter with a lifetime $\lesssim 0.5$ Gyr (Poulin et al. 2019). Mid- z models cannot change late-time constraints like γ -ray and CC, which are not very constraining in H_0 but push toward lower Ω_m values. They might be able to change and loosen the cosmic-age bound, but this requires the cosmic expansion to be slower during the mid-redshift range (compared to a standard evolution of H) to compensate for the rising of today’s H_0 . If this decrease of the earlier cosmic expansion extended to the very early universe (before recombination), it would conflict with the CMB and late-time BAO observations, as slower cosmic expansion before recombination makes the sound horizon even larger.

Low- z models (L) refer to those have some non-standard physics during a redshift range relevant for most of the late-time observations considered here (i.e. $z \lesssim 6$), but reduce to a standard cosmological model at higher redshifts. Recent examples are interacting dark energy (Pan et al. 2019), a rolling scalar field (Agrawal et al. 2019) and nonlocal modified gravity (Belgacem et al. 2018). Most of the constraints here would be affected in some way by late-time evolution; however, it has been argued that late-time models are not able to reconcile the Hubble constant tension (Aylor et al. 2019; Evslin et al. 2018). Observations such as BAO and SNIa that

² This does not mean the two datasets are observationally dependent. We did not use any prior information from CMB as in the BAO constraints, but rather used BBN data to constrain $\Omega_b h^2$.

probe the late-time background evolution can further constrain models of this category.

While the above models can alter many of the constraints, some proposals suggest some **local/environmental factors** ($z \lesssim 0.03$) (E) can bias the local determinations. This would mean the locally measured H_0 cannot be interpreted as the global Hubble constant of the homogeneous universe. An example is a local underdense region (Lombriser 2019; Shanks et al. 2019). Recent studies have shown observational evidence supporting a small-scale local underdense region (Boehringer et al. 2019; Pustilnik et al. 2019), though it has been argued that the likelihood for a local void to substantially affect the local measurement may be low (Kenworthy et al. 2019). These local factors do not pose a problem to the standard Λ CDM model at large scales, but instead point to the need for a more detailed description of our local environment to account for such a systematic effect that can shift all local measurements in the same way. If all local measurements produce high values of H_0 , it would favor such a local/environmental-factor explanation over systematic effects that may be unique to each observation.

Comparing different local measurements is therefore important. The recent TRGB-based (tip of the red giant branch) local measurement (Freedman et al. 2019), giving $H_0 = 69.8 \pm 1.9$ km/s/Mpc, is more consistent with Planck than with CV SN while still being in some tension with both. Other authors have revisited this result and found a higher value, $H_0 = 72.4 \pm 1.9$ km/s/Mpc (Yuan et al. 2019). The recent Mira-based local measurement also gives a relatively high $H_0 = 73.3 \pm 3.9$ km/s/Mpc (Huang & et al 2019). While there are conflicts among the distance-ladder based methods, they overall favor a higher H_0 . But as they are all based on Type Ia supernovae (using different calibrations), it is possible that they could share some common systematic effect(s) or biases due to some other physical considerations. For instance, Desmond et al. (2019) have proposed that screened fifth forces may affect the calibration of Type Ia supernovae. There are local determinations that do *not* require the distance ladder or Type Ia supernovae, such as the megamaser cosmology project (MCP) (Reid et al. 2009) and the standard siren multimessenger method (The LIGO Scientific Collaboration et al. 2019). The current publicly available joint result from MCP is 69.3 ± 4.2 km/s/Mpc,³ a relatively weak constraint in between the Planck and the CV SN results. The multimessenger constraint is still too weak to play a significant role. Note that although the TDSL technique is relatively insensitive to the underlying cosmological model, it is not a local measurement⁴. Going forward, we anticipate that new observables will be key to confirming or ruling out any possible environmental effects.

4. DISCUSSION

³ See <https://safe.nrao.edu/wiki/bin/view/Main/MegamaserCosmologyProject>.

⁴ By local measurements, we refer to methods that are *only* based on the Hubble-Lemaître law and small- z ($z \lesssim 0.02$) observations.

We present these results as an exploration of the range of possibilities for approaching tensions among these disparate datasets. It should be noted that our numerical analysis does not include the cosmic-age bound, since single-sided constraints cannot be considered in the moment-based IOI formalism. However, considering these bound can only strengthen our conclusion, since the cosmic-age bound shown in Figure 1 excludes the regions overlapped by CV SN with SNIa and DES, and that with BAO Low. As mentioned earlier, the recent TRGB-based determination of H_0 is lower than that of CV SN (Freedman et al. 2019). If we replace CV SN with this result and redo our numerical analysis, the IOI and all \mathcal{O}_j 's are significantly reduced; see the last row in Table 1. Recently, Ivanov et al. (2019) reanalysed the galaxy power spectrum (embedding BAO) at $z_{\text{eff}} = 0.38$ and 0.61 using a perturbation theory method that accounts for non-linear clustering and a range of other effects. Their constraint on the H_0 - Ω_m plane also falls into the guiding circle in Figure 1.

It is also worth pointing out that we do not find the constraint obtained from the current publicly available TDSL data (only four systems) to be an outlier, even though its mean value of H_0 is relatively high. There are three reasons: (1) The uncertainty of H_0 of that TDSL constraint is relatively large. (2) A multi-constraint comparison checks how compatible each constraint is with all other constraints, not just with Planck. And (3) again, our numerical analysis does not include the cosmic-age bound, which would make the TDSL constraint more outlying. The most recent joint analysis of six TDSL systems gives an even higher H_0 (Wong et al. 2019). While this dataset is not yet publicly available, we expect it will be more outlying compared with other non-local constraints. This may to some extent weaken our conclusion, though some authors have suggested that the H_0 measurement using the TDSL technique can be affected due to the mass-sheet degeneracy and the issue may be more complicated than is assumed (Gomer & Williams 2019). We will update our analysis when their new data become publicly available.

A caveat in our investigation is that all observations are treated upon the same footing in the sense that not any one of them is considered as more reliable than any other. In practice, some results may be more or less vulnerable to systematic effects. In particular, cosmic chronometers and γ -ray attenuation put pressure on high- and mid- z models that try to resolve the H_0 tension and thus warrant further study. In addition, constraining the cosmic age is promising to constitute a strong test to high- z (and likely also mid- z) models. In fact, any objects or methods that confirm a cosmic age $\gtrsim 13.5$ Gyr since $z = 100$ can rule out all high- z solutions to the current H_0 tension.

5. CONCLUSIONS

It is very beneficial to compare constraints individually in the H_0 - Ω_m space when investigating the H_0 tension. It allows us to more robustly see how different constraints behave

in the standard Λ CDM model as well as to more easily tell whether a nonstandard model can reconcile all constraints.

We have performed a systematic comparison of various constraints from different observations in the H_0 - Ω_m space based on the standard Λ CDM model. Most constraints consistently overlap along different degeneracy directions on some common region in the H_0 - Ω_m plane centered around the general vicinity of (68.5, 0.3). The fact that the Cepheid-based local determination of H_0 does not overlap with such a common region suggests that the main driver of the tension may be supposed to be the local measurement(s). It is difficult for high- z , mid- z or low- z nonstandard evolution models to reconcile the constraints of all the considered observations as they stand. Confirming the results from γ -ray attenuation and cosmic chronometers as well as the lower limit of cosmic age can rule out high- and mid- z models that try to resolve the current H_0 tension. Thus, the analysis we have performed here prefers a solution that alters the local determination, as opposed to a modification of Λ CDM on large scales. Such a solution need not be a systematic effect in one dataset, but could take the form of some previously undiscovered anomaly in our local cosmic environment, shifting all local determinations of H_0 to higher values.

In the future, there will be more and more independent methods to constrain the cosmic evolution. For instance, observing the redshift drift will allow us to directly detect the

real-time cosmic expansion (Loeb 1998). BAO constraints will be improved from the line-intensity mapping of emission from star-forming galaxies (Bernal et al. 2019) and the next-generation galaxy surveys (Bengaly et al. 2019). The observed drop-off in the abundance of $\gtrsim 45M_\odot$ black holes can be used to probe cosmic expansion by making binary black hole mergers “standardizable” (Farr et al. 2019). Velocity-induced acoustic oscillations, a standard ruler that can be seen in 21-cm power spectrum, provide a way to probe the background evolution at cosmic dawn (Muñoz 2019). And standard siren multimessengers provide another way to measure H_0 . Comparing them all in the H_0 - Ω_m space can help us to more easily discover the fundamental cause of the Hubble constant tension.

It is exciting to see whether the current Hubble constant tension is leading us to another new understanding of the universe. We hope that this analysis motivates a new way of considering the various cosmological constraints and a different perspective on viewing such a tension.

ACKNOWLEDGMENTS

We thank Alberto Domínguez Díaz for providing the MCMC chain of the analysis to the γ -ray attenuation data, and Mustapha Ishak and Brian Schmidt for useful comments on an earlier draft.

REFERENCES

- Abbott, T. M. C., et al. 2018, *PhRvD*, 98, 043526, doi: [10.1103/PhysRevD.98.043526](https://doi.org/10.1103/PhysRevD.98.043526)
- Addison, G. E., Huang, Y., Watts, D. J., et al. 2016, *ApJ*, 818, 132, doi: [10.3847/0004-637X/818/2/132](https://doi.org/10.3847/0004-637X/818/2/132)
- Agrawal, P., Obied, G., & Vafa, C. 2019. [arXiv:1906.08261](https://arxiv.org/abs/1906.08261)
- Alam, S., et al. 2017, *MNRAS*, 470, 2617, doi: [10.1093/mnras/stx721](https://doi.org/10.1093/mnras/stx721)
- Ata, M., et al. 2018, *MNRAS*, 473, 4773, doi: [10.1093/mnras/stx2630](https://doi.org/10.1093/mnras/stx2630)
- Aylor, K., Joy, M., Knox, L., et al. 2019, *The Astrophysical Journal*, 874, 4, doi: [10.3847/1538-4357/ab0898](https://doi.org/10.3847/1538-4357/ab0898)
- Belgacem, E., Dirian, Y., Foffa, S., & Maggiorè, M. 2018, *JCAP*, 2018, 002, doi: [10.1088/1475-7516/2018/03/002](https://doi.org/10.1088/1475-7516/2018/03/002)
- Bengaly, C. A. P., Clarkson, C., & Maartens, R. 2019. [arXiv:1908.04619](https://arxiv.org/abs/1908.04619)
- Bernal, J. L., Breyse, P. C., & Kovetz, E. D. 2019, *arXiv e-prints*, [arXiv:1907.10065](https://arxiv.org/abs/1907.10065). [arXiv:1907.10065](https://arxiv.org/abs/1907.10065)
- Beutler, F., et al. 2011, *MNRAS*, 416, 3017, doi: [10.1111/j.1365-2966.2011.19250.x](https://doi.org/10.1111/j.1365-2966.2011.19250.x)
- Blomqvist, M., et al. 2019, *A&A*, 629, A86, doi: [10.1051/0004-6361/201935641](https://doi.org/10.1051/0004-6361/201935641)
- Boehringer, H., Chon, G., & Collins, C. A. 2019. [arXiv:1907.12402](https://arxiv.org/abs/1907.12402)
- Bond, H. E., Nelán, E. P., VandenBerg, D. A., Schaefer, G. H., & Harmer, D. 2013, *ApJ*, 765, L12, doi: [10.1088/2041-8205/765/1/L12](https://doi.org/10.1088/2041-8205/765/1/L12)
- Cooke, R. J., Pettini, M., & Steidel, C. C. 2018, *ApJ*, 855, 102, doi: [10.3847/1538-4357/aaab53](https://doi.org/10.3847/1538-4357/aaab53)
- Desmond, H., Jain, B., & Sakstein, J. 2019, *PhRvD*, 100, 043537, doi: [10.1103/PhysRevD.100.043537](https://doi.org/10.1103/PhysRevD.100.043537)
- Domínguez, A., et al. 2019. [arXiv:1903.12097](https://arxiv.org/abs/1903.12097)
- Evslin, J., Sen, A. A., & Ruchika. 2018, *PhRvD*, 97, 103511, doi: [10.1103/PhysRevD.97.103511](https://doi.org/10.1103/PhysRevD.97.103511)
- Farr, W. M., Fishbach, M., Ye, J., & Holz, D. 2019. [arXiv:1908.09084](https://arxiv.org/abs/1908.09084)
- Freedman, W. L., et al. 2019, *ApJ*, 882, 34, doi: [10.3847/1538-4357/ab2f73](https://doi.org/10.3847/1538-4357/ab2f73)
- Gomer, M. R., & Williams, L. L. R. 2019. [arXiv:1907.08638](https://arxiv.org/abs/1907.08638)
- Hamana, T., et al. 2019. [arXiv:1906.06041](https://arxiv.org/abs/1906.06041)
- Hinshaw, G., et al. 2013, *ApJS*, 208, 19, doi: [10.1088/0067-0049/208/2/19](https://doi.org/10.1088/0067-0049/208/2/19)
- Huang, C. D., & et al. 2019. [arXiv:1908.10883](https://arxiv.org/abs/1908.10883)
- Ivanov, M. M., Simonović, M., & Zaldarriaga, M. 2019, *arXiv e-prints*, [arXiv:1909.05277](https://arxiv.org/abs/1909.05277). [arXiv:1909.05277](https://arxiv.org/abs/1909.05277)
- Joudaki, S., et al. 2019. [arXiv:1906.09262](https://arxiv.org/abs/1906.09262)
- Kenworthy, W. D., Scolnic, D., & Riess, A. 2019, *ApJ*, 875, 145, doi: [10.3847/1538-4357/ab0ebf](https://doi.org/10.3847/1538-4357/ab0ebf)

- Kreisch, C. D., Cyr-Racine, F.-Y., & Doré, O. 2019. [arXiv:1902.00534](#)
- Lewis, A., & Bridle, S. 2002, *PhRvD*, 66, 103511, doi: [10.1103/PhysRevD.66.103511](#)
- Lin, W., & Ishak, M. 2017, *Phys. Rev. D*, 96, 023532, doi: [10.1103/PhysRevD.96.023532](#)
- Lin, W., & Ishak, M. 2019. [arXiv:1909.10991](#)
- Loeb, A. 1998, *The Astrophysical Journal*, 499, L111, doi: [10.1086/311375](#)
- Lombriser, L. 2019. [arXiv:1906.12347](#)
- Muñoz, J. B. 2019, *Phys. Rev. Lett.*, 123, 131301, doi: [10.1103/PhysRevLett.123.131301](#)
- O'Malley, E. M., Gilligan, C., & Chaboyer, B. 2017, *The Astrophysical Journal*, 838, 162, doi: [10.3847/1538-4357/aa6574](#)
- Pan, S., Yang, W., Di Valentino, E., Saridakis, E. N., & Chakraborty, S. 2019. [arXiv:1907.07540](#)
- Planck Collaboration, Aghanim, N., et al. 2016, *A&A*, 594, A11, doi: [10.1051/0004-6361/201526926](#)
- . 2018. [arXiv:1807.06209](#)
- Poulin, V., Smith, T. L., Karwal, T., & Kamionkowski, M. 2019, *PhRvL*, 122, 221301, doi: [10.1103/PhysRevLett.122.221301](#)
- Pustilnik, S. A., Tepliakova, A. L., & Makarov, D. I. 2019, *MNRAS*, 482, 4329, doi: [10.1093/mnras/sty2947](#)
- Reid, M. J., Braatz, J. A., Condon, J. J., et al. 2009, *ApJ*, 695, 287, doi: [10.1088/0004-637X/695/1/287](#)
- Riess, A. G., Casertano, S., Yuan, W., Macri, L. M., & Scolnic, D. 2019, *The Astrophysical Journal*, 876, 85, doi: [10.3847/1538-4357/ab1422](#)
- Ross, A. J., Samushia, L., Howlett, C., et al. 2015, *MNRAS*, 449, 835, doi: [10.1093/mnras/stv154](#)
- Sandage, A. R. 1970, *Physics Today*, 23, 34, doi: [10.1063/1.3021960](#)
- Schlaufman, K. C., Thompson, I. B., & Casey, A. R. 2018, *The Astrophysical Journal*, 867, 98, doi: [10.3847/1538-4357/aadd97](#)
- Scolnic, D. M., et al. 2018, *ApJ*, 859, 101, doi: [10.3847/1538-4357/aab9bb](#)
- Shanks, T., Hogarth, L. M., & Metcalfe, N. 2019, *MNRAS*, 484, L64, doi: [10.1093/mnras/sly239](#)
- The LIGO Scientific Collaboration, the Virgo Collaboration, Abbott, B. P., et al. 2019. [arXiv:1908.06060](#)
- Wibking, B. D., et al. 2019. [arXiv:1907.06293](#)
- Wong, K. C., et al. 2019. [arXiv:1907.04869](#)
- Yu, H., Ratra, B., & Wang, F.-Y. 2018, *ApJ*, 856, 3, doi: [10.3847/1538-4357/aab0a2](#)
- Yuan, W., Riess, A. G., Macri, L. M., Casertano, S., & Scolnic, D. 2019. [arXiv:1908.00993](#)